

Topological phase transition in a two-dimensional nematic n -vector model: A numerical study

H. Kunz

*Ecole Polytechnique Fédérale de Lausanne, Institut de Physique Théorique, PHB-Ecublens,
CH-1015 Lausanne, Switzerland*

G. Zumbach

*Max-Planck-Institut für Festkörperforschung, Heisenbergstrasse 1, D-7000 Stuttgart 80, Germany
(Received 19 June 1991; revised manuscript received 2 December 1991)*

A Monte Carlo study, based on a cluster algorithm, is made of the two-dimensional $\mathbb{R}P^{n-1}$ model. Introducing various types of order parameters, we find strong evidence for a topological phase transition, driven by a condensation of defects. For $n=3$, the model describes a nematic liquid crystal. In this case, the transition is associated to a divergence of the correlation length and of the susceptibility, and a cusp in the specific heat. The results for $n=40$ are compared with the analytical ones for $n=\infty$. The critical temperature is correctly reproduced, but the detailed nature of the transition is not. Crossover phenomena are detected, which reflect the noncommutativity of the $n=\infty$ and the thermodynamic limit for some observables.

I. INTRODUCTION

Two-dimensional models of physical systems continue to attract attention, both in statistical mechanics and in field theory, particularly those that produce a phase transition and related critical phenomena. The existence of a phase transition in these systems often appears to be crucially related to the commutative (Abelian) nature of the symmetry group. The Ising and X - Y models provide standard examples. Both transitions, however, can also be seen as driven by a condensation of defects: the Peierls droplets in the Ising case and the vortices in the XY model, as was shown by Berezinski¹ and Kosterlitz-Thouless.² In contrast, when the symmetry group is non-Abelian, as in the $O(3)$ Heisenberg model and its generalizations, there exists much evidence, both theoretical³ and numerical,⁴ against any type of transition. However, to disentangle the effects of the symmetry group and the homotopy group that classify topological stable defects in order to determine whether a phase transition does exist appears to be a difficult task. This became especially clear when recently Lau and Dasgupta⁵ showed, in a numerical study of the three-dimensional $O(3)$ Heisenberg model, that in the absence of point defects the transition disappeared. The system remains in its low-temperature phase, and spin-wave interactions cannot disorder it over a large length scale. This result, as emphasized by these authors, calls into question a description of the model by its continuum limit: the nonlinear σ model, basic to all studies of the two-dimensional case. It is therefore important to determine whether the existence of stable defects in a two-dimensional system with a continuous noncommutative symmetry group can induce a phase transition without long-range order.

With this purpose in mind we have undertaken a numerical and analytical study of a nematic n -vector model, which is called the $\mathbb{R}P^{n-1}$ model, for reasons to be given later. In this lattice model, to each lattice site is attached

a direction in n -dimensional space. There is an interaction between nearest neighbors, which tends to make the corresponding directions parallel. In the $n=3$ case, we can think of these directions as representing very elongated molecules in the usual three-dimensional space. The model should therefore describe qualitatively the nematic liquid-crystal phase transition; it has been introduced for this purpose by Lebwohl and Lasher.⁶ In the liquid-crystal context, the defects are called disclination lines. The Hamiltonian of the model can be written as

$$H = - \sum_{x,\mu} (\sigma(x), \sigma(x, +\mu))^2, \quad (1.1)$$

where the variables $\sigma(x)$ are n -component unit vectors at sites x of a square lattice and μ denotes the two directions of the lattice, $(\sigma(x), \sigma(y))$ denotes the scalar product of the vector $\sigma(x)$ with the vector $\sigma(y)$. The $n=2$, case of the model is equivalent to the XY model as can be seen by using the trigonometric identity $\cos^2\theta = \frac{1}{2}[1 + \cos(2\theta)]$.

Values of $n \geq 4$ are of theoretical interest, especially since the limiting case $n=\infty$ is solvable.⁷ The model is particularly interesting for the following reasons. It possesses, like the usual n -vector model, the symmetry group $O(n)$, which is noncommutative for $n \geq 3$. It enjoys local gauge invariance, with group \mathbb{Z}_2 . But this simply reflects the fact that, with a Hamiltonian written in form (1.1), we have described a direction by a unit vector $\sigma(x)$ and that the vector $-\sigma(x)$ describes the same direction. At each lattice site, we have therefore attached the manifold of directions in n -dimensional space. This manifold is known as the real projective space in n dimensions by mathematicians, in short $\mathbb{R}P^{n-1}$. This manifold is equivalent to the unit $(n-1)$ -sphere S^{n-1} with opposite points identified. Globally these manifolds differ, but locally they are the same. If we attached a unit $(n-1)$ -sphere to each lattice point, we would have constructed the familiar n -component model. In physical terms, the local identity of their manifolds means that the spin-wave

excitations of the \mathbb{RP}^{n-1} and S^{n-1} models are the same. This is seen most clearly by taking the continuum limit of both models. The Hamiltonian becomes

$$H = \frac{a}{2} \sum_{\mu=1}^2 \int d^2x (\partial_{\mu}\sigma, \partial_{\mu}\sigma)(x), \quad (1.2)$$

where $a=1$ for S^{n-1} model and $a=2$ for the \mathbb{RP}^{n-1} model.

The Hamiltonian is that of the usual nonlinear σ model⁸ and describes spin-wave interactions in both the S^{n-1} and \mathbb{RP}^{n-1} models at long wavelengths. A renormalization-group treatment of the nonlinear σ model predicts no phase transition in two dimensions and a continuous one in three dimensions for $n \geq 3$. Monte Carlo studies of the \mathbb{RP}^{n-1} model, however, have consistently observed a first-order phase transition in three dimensions.^{6,9,10} This indicates either a breakdown of the $2+\epsilon$ expansion in this case, when $\epsilon \approx 1$, or the possibility of a genuine phase transition in two dimensions. What could the origin be of such a phase transition and what is the possible problem with the continuum limit described by the nonlinear σ model Hamiltonian (1.2)? The problem is the existence of defects, present in the \mathbb{RP}^{n-1} model and absent in the usual n -component model, when $n \geq 3$. Physically, they are disclination lines. Mathematically, their existence is related to the fact that the sphere with opposite points identified is topologically different from the usual sphere. One is tempted therefore to conclude that these defects and their interaction are the driving mechanism of the transition in the three-dimensional case, and might lead to a genuine phase transition in two dimensions. Solomon¹¹ already suggested the existence of a defect-mediated phase transition in two dimensions and found some evidence for it. Subsequent studies of the \mathbb{RP}^2 model¹² or related ones^{11,13} concluded in favor of some kind of phase transition in two dimensions, whereas some others did not.¹⁰

The existence of a first-order phase transition with latent heat, in the limiting case $n = \infty$, even in two dimension,⁷ prompted us to reconsider the problem. On the other hand the recent availability of cluster algorithms, which have successfully overcome the critical slowing down in the usual n -vector model, suggested that the situation could also be clarified from the numerical point of view. Using the Monte Carlo algorithm due to Wolff¹² and the recently available method of Ferrenberg and Swendsen,¹⁴ we have found strong evidence for a topological phase transition, driven by defects in these models. In the liquid-crystal with $n=3$, this transition is associated with a divergence of the correlation length and a cusp in the specific heat. Much of the evidence for a phase transition also comes from the study of two additional order parameters, one of which appears to have a discontinuity at the transition point.

We also studied the model for large values of n ($n=40$), in order to compare with analytic theoretical results known for $n = \infty$ case. The results are discomforting. Whereas the critical temperature is close to the $n = \infty$ theoretical value, the internal energy shows a crossover behavior. It seems to have an abrupt discontinuity for small sample sizes in agreement with the

$n = \infty$ theoretical result, but this discontinuity becomes less abrupt with increasing system. It appears therefore that the limit $n = \infty$ and the thermodynamic limit do not commute in the two-dimensional case. Motivated by these results, we have reconsidered the $n = \infty$ limit from a more rigorous point of view than before. We have proven that the thermodynamic limit and the $n = \infty$ limit commute for the free energy and confirmed the previous result for this quantity. This can partially explain the numerical observations.

Finally, we would like to mention that the \mathbb{RP}^{n-1} model is the simplest member of a large class of the nonlinear σ models, the so-called Grassmanian models. At each space point we would attach the manifold of k planes in n -dimensional space $O(n+k)/[O(n) \times O(k)]$. Such models have been mostly analyzed in the continuum limit⁸ where they can be studied in $2+\epsilon$ dimensions. The noncompact Grassmanian model $O(n,n)/[O(n) \times O(n)]$ describes the localization transition, in the limit $n=0$, as shown by Wegner.¹⁵ Lattice versions of these models can be constructed.¹⁰ They all undergo a first-order phase transition at the mean-field level.¹⁰ We have shown that, in the $n = \infty$ limit, keeping k fixed, they undergo a first-order transition in any dimension larger than two, because in this limit they are basically k copies of the \mathbb{RP}^{n-1} model.

Some of these models also possess a fundamental homotopy group \mathbb{Z}_2 , and therefore defects of the same kind as those of the \mathbb{RP}^{n-1} models. It would be quite interesting, in our opinion, to analyze the role of these defects, which are consistently neglected in the treatment of these models in their continuum limit. A brief summary of these results has been presented in a separate publication.¹⁶

II. THE \mathbb{RP}^{n-1} MODEL: BASIC OBSERVABLES AND ORDER PARAMETERS

There are two possible descriptions of the model, an intrinsic and an extrinsic one, both quite useful. An intrinsic description of a direction at the lattice site x is provided by a one-dimensional projector, i.e., an $n \times n$ symmetric matrix $P(x)$, such that $P^2(x)=P(x)$ and $\text{tr}P(x)=1$. In these variables the Hamiltonian of our system is given by

$$H[P] = \frac{1}{2} \sum_{\mu,x} \text{tr}[(\partial_{\mu}P)^2(x)], \quad (2.1)$$

where

$$(\partial_{\mu}P)(x) = P(x+\mu) - P(x) \quad (2.2)$$

and μ denotes one of the d unit vectors of the d -dimensional cubic lattice with unit lattice spacing. The volume will be a cube of size L , and we will use periodic boundary conditions. $N=L^d$ will denote the total number of sites.

We can, however, use an extrinsic description of the direction by attaching to it a unit vector $\sigma(x)$, i.e.,

$$\sigma^2(x) = 1 \quad (2.3)$$

and taking for the projector $P(x)$:

$$P(x): P_{\alpha\beta}(x) = \sigma_\alpha(x)\sigma_\beta(x), \quad \alpha, \beta \in \{1, 2, \dots, n\}. \quad (2.4)$$

In this notation, the Hamiltonian becomes

$$H[\sigma] = - \sum_{\mu, x} (\sigma(x), \sigma(x+\mu))^2 + dL^d. \quad (2.5)$$

In this form, besides the global $O(n)$ symmetry, the Hamiltonian is invariant under the local gauge group \mathbb{Z}_2 , corresponding to $\sigma(x) \rightarrow \pm\sigma(x)$. The average value of an observable will be given by

$$\langle A \rangle = \frac{\int d\nu(\sigma) e^{-\beta H[\sigma]} A(\sigma)}{\int d\nu(\sigma) e^{-\beta H[\sigma]}}, \quad (2.6)$$

where

$$d\nu(\sigma) = c^{L^d} \int \prod_x \delta(\sigma^2(x) - 1) d\sigma(x), \quad (2.7)$$

and the constant c is chosen so that

$$\int d\nu(\sigma) = 1. \quad (2.8)$$

The thermodynamic quantities of interest to us are the following: the energy per link,

$$h = \frac{1}{dL^d} \langle H[P] \rangle, \quad (2.9)$$

the specific heat,

$$C_v = \frac{\partial}{\partial T} \langle H[P] \rangle, \quad (2.10)$$

the scalar susceptibility,

$$\chi = \frac{1}{L^d} \text{tr} \left[\left\langle \left[\sum_x P(x) \right]^2 \right\rangle - \left\langle \sum_x P(x) \right\rangle^2 \right], \quad (2.11)$$

and, since

$$\langle P(x) \rangle = \frac{1}{n}, \quad (2.12)$$

we also have

$$\chi = \left\langle \sum_x (\sigma(0), \sigma(x))^2 \right\rangle - \frac{L^d}{n}. \quad (2.13)$$

If one is interested in the usual long-range order, one can introduce an order parameter defined locally as

$$m(x) = \frac{n\sigma_1^2(x) - 1}{n-1} \quad (2.14)$$

if the ordering field has been put in the direction 1. The corresponding susceptibility χ_1 given by

$$\chi_1 = \frac{1}{L^d} \sum_{x,y} \langle m(x)m(y) \rangle \quad (2.15)$$

is related to the scalar susceptibility by

$$\chi = \chi_1 \frac{n-1}{2} \left[n+1 - \frac{2}{n} \right], \quad (2.16)$$

as can be seen, by using the rotational invariance. We

will, however, be concerned here with the two-dimensional system, in which the usual order parameter $\langle m(x) \rangle$ vanishes as a consequence of a Mermin-Wagner-type theorem.

In order to define a correlation length ξ , we consider the Fourier transform of the two-point correlation function

$$G(k) = \sum_x e^{ik \cdot x} \left[\langle (\sigma(0), \sigma(x))^2 \rangle - \frac{1}{n} \right]. \quad (2.17)$$

In the infinite system, when the correlation function $g(x) = \langle (\sigma(0), \sigma(x))^2 \rangle - 1/n$ decays exponentially, we will have

$$[G(k)]^{-1} = \chi^{-1} [1 + k^2 \xi^2 + O(k^4)] \quad (2.18)$$

with

$$\xi^2 = \frac{1}{2} \frac{\sum_x x^2 g(x)}{\sum_x g(x)} \quad (2.19)$$

and

$$\chi = G(0) = \sum_x g(x). \quad (2.20)$$

In the numerical study, we proceed as follows. We compute χ from (2.11) and then define the correlation length by the equation

$$[G(k)]^{-1} = \chi^{-1} [1 + k^2 \xi^2] \quad (2.21)$$

by choosing $K = (0, 2\pi/L)$ and by computing $G(k)$ from Eq. (2.17). This correlation length ξ_L can be proved to tend to ξ given by (2.19), when L tends to infinity, if $g(x)$ decays fast enough.

One of the most interesting features of the $\mathbb{R}P^{n-1}$ model is the existence of topologically stable defects even in two dimensions because $\pi_1(\mathbb{R}P^{n-1}) = \mathbb{Z}_2$ when $n \geq 3$. These defects are well known in liquid-crystal theory as disclination lines, in the three-dimensional case. In two dimensions they are point defects. These defects are usually defined in the continuum limit, where the director field $P(x)$ varies smoothly except at the defects. On the lattice, however, the typical configurations on a small length scale appear to be rather wild. We need therefore to interpolate the lattice configurations. We proceed as follows: to the bond (x, y) we associate the shortest geodesic connecting the vectors $\sigma(x)$ and $\sigma(y)$ on the unit $(n-1)$ sphere. In this way we can obtain a map from a closed loop \mathcal{L} on the lattice to a loop on the manifold $\mathbb{R}P^{n-1}$. The homotopy class of this map is given by

$$w(\mathcal{L}) = \prod_{(xy) \in \mathcal{L}} \text{sgn}(\sigma(x), \sigma(y)) = \text{sgn tr} \prod_{x \in \mathcal{L}} P(x), \quad (2.22)$$

the product of projectors being an ordered one. If $W(\mathcal{L}) = +1$ [$W(\mathcal{L}) = -1$], then the loop encloses an even (odd) number of defects. This definition works for all configurations except for a set of measure zero, corresponding to vanishing values of $(\sigma(x), \sigma(y))$. Moreover, it preserves the multiplicative structure of the \mathbb{Z}_2 group, i.e., $W(\mathcal{L} \cdot \mathcal{L}') = W(\mathcal{L})W(\mathcal{L}')$, a homomorphism, and

agrees with the usual notion in the continuum limit. We can then define the density of defects by

$$D = \frac{1}{2} [1 - \langle W(\partial P) \rangle], \quad (2.23)$$

where ∂P is the boundary of a plaquette P of the lattice. It vanishes in the ground state and should show an exponential behavior $\exp(-\beta E_0)$ at low temperatures, E_0 being an activation energy for a pair of defects. Finally, we expect it to increase with temperature.

We can also measure the fluctuation of the number of defects. It is defined by

$$\chi_D = \frac{1}{L^d} \left[\left\langle \left[\sum_x D(x) \right]^2 \right\rangle - \left\langle \sum_x D(x) \right\rangle^2 \right], \quad (2.24)$$

where $D(x) = \frac{1}{2} [1 - W(\partial P(x))]$ takes the value 1 if there is a defect at the center of the plaquette $P(x)$ and 0 otherwise. We call this quantity the susceptibility of defects.

We can take advantage of the periodic boundary conditions to define a topological order parameter measuring the pairing of the defects. Indeed, the lattice can be thought of as a lattice on a torus. If we move vertically, for example, from one boundary of the square to the other, we describe a loop \mathcal{L} on the torus and to this loop corresponds the element of the homotopy group $W(\mathcal{L})$. We therefore define as our *topological order parameter* the quantity

$$\mu = \langle W(\mathcal{L}) \rangle. \quad (2.25)$$

Note that this loop is not homotopically equivalent to the one used in the definition of the defects density D . At high temperatures it vanishes exponentially in the length

$$\begin{aligned} \Sigma = & -L^{-d} \sum_x \langle [(\sigma(x), \sigma(x + \mu_1))(\sigma(x), J^2 \sigma(x + \mu_1)) + (\sigma(x), J\sigma(x + \mu_1))^2] \rangle \\ & - 2\beta L^{-d} \left\langle \left[\sum_x (\sigma(x), \sigma(x + \mu_1))(\sigma(x), J\sigma(x + \mu_1)) \right]^2 \right\rangle, \end{aligned} \quad (2.30)$$

where J is the generator of the rotation in the (1,2) plane.

The quantity Σ is our desired order parameter that we will call the *rotational-rigidity modulus*. This quantity vanishes in the thermodynamic limit when the correlation functions decay exponentially, i.e., at high temperatures. In the ordered phase, which appears in three dimensions, it is nonzero. We have computed it in the limit $n = \infty$, and one finds that, indeed,

$$\Sigma = 0 \quad \text{if } T > T_c, \quad (2.31)$$

$$\Sigma = \frac{2}{n} \left[1 + \sqrt{1 - 1/d\beta} - \frac{\bar{\Lambda}}{2\beta} \right] \quad \text{if } T < T_c,$$

where

$$\bar{\Lambda} = \int_0^{2\pi} \prod_{\mu=1}^d \frac{d\theta_\mu}{2\pi} \frac{1}{d - \sum_{\mu} \cos\theta_\mu} \quad (2.32)$$

when the space dimensionality $d \geq 3$. This quantity makes a jump at T_c .

L . At low temperatures, if we have a ‘‘phase’’ in which defects are absent or paired, this quantity should be nonzero even in the thermodynamic limit.

Finally, it appears useful to introduce an order parameter which measures the rigidity of the system with respect to rotations. In the case of the XY model, this is the helicity modulus^{17,18} which is proportional to the superfluid density. When the symmetry group is non-Abelian, or in the RP^{n-1} model, we propose to define it as follows: Let

$$\begin{aligned} H(g) = & \sum_{x,y} \text{tr}[P(x)g_\mu P(x + \mu)g_\mu^{-1}] \\ = & - \sum_x (\sigma(x), g_\mu \sigma(x + \mu))^2 \end{aligned} \quad (2.26)$$

be a modified Hamiltonian where g_μ is a rotation of angle θ_μ/L in the (1,2) plane in the spin space, for example. Choosing $\theta_\mu = \delta_{\mu,1}\theta$, we can compute the free-energy increment due to this rotation

$$F(\theta) - F(0) = \frac{-1}{\beta} \ln \left[\frac{Z(g)}{Z(1)} \right], \quad (2.27)$$

where

$$Z(g) = \int d\nu(\sigma) e^{-BH(g)} \quad (2.28)$$

is the partition function for a system described by the Hamiltonian $H(g)$. For small angles θ , we get

$$F(\theta) - F(0) = \theta^2 \Sigma + O(\theta^4), \quad (2.29)$$

where

In contrast, in the two-dimensional case one finds that Σ vanishes identically when $n = \infty$, despite the existence of a first-order thermodynamic phase transition. We interpret this as the result of the exponential decay of correlation functions, which occur in this case. We conclude, therefore, that this order parameter can be expected to be nonzero, even in the absence of long-range order, if the correlation functions show a sufficiently slow power-law decay, like the helicity modulus in the two-dimensional XY model.

III. NUMERICAL TECHNICALITIES

We began simulations with the usual local update in the manner of the Metropolis algorithm, sweeping in temperature. The results were very poor because of the huge autocorrelation time of this algorithm. So, two key ingredients for the success of the simulations are the recently available method of Ferrenberg and Swendsen¹⁴ and a nonlocal update for σ due to Wolff.⁴ The Ferrenberg-Swendsen method allows us to do Monte Car-

lo (MC) simulations for a set of temperatures and then to combine the different histograms in order to minimize the error on our knowledge of the density of state. Then, we can compute the average of various quantities in function of β . Moreover, we can add simulations as we wish in order to reduce the errors, and this method does not depend on the update algorithm. The second essential ingredient is a cluster update. Recently, Wolff^{4,13} designed such an algorithm for the $O(n)$ nonlinear σ model, and he checked that it is ergodic and satisfies the detailed-balance condition. It is easy to modify the activating probability so as to satisfy the detailed-balance condition for the RP^{n-1} model. Briefly, the update in the RP^{n-1} case runs as follows.

- (1) Take a random unit vector $r \in \mathbb{R}^n$, and define $\sigma(x)' = \sigma(x) - 2(\sigma(x), r)r$.
- (2) Activate bonds (x, y) of the lattice with a probability

$$p(x, y) = 1 - \exp(\min\{0, 4\beta(\sigma'_x, r)(\sigma_y, r) \times [(\sigma'_x, \sigma_y) - (\sigma'_x, r)(\sigma_y, r)]\}) \quad (3.1)$$

and construct the different clusters of activated bonds

- (3) Choose at random one or many clusters, and flip the corresponding spins according to $\sigma(x) \rightarrow \sigma'(x)$.

As described above, one update will take a time of order L^d . But according to Wolff, we can modify the algorithm slightly by constructing only one flipped cluster attached to a random starting point x_0 , which now will take a time of order of the flipped cluster size. In order to attain effectively the optimal bound, we should keep two representations of the cluster, one as a list of points with their associated coordinates, and one as a table of occupied sites. The list of points is divided into the point already in the cluster, and the points at the border where the cluster is still growing. When the last list is empty, the construction of one cluster is finished. However, in the low-temperature phase, the correlation length as well as the cluster size is of order of the sample size. This is very inefficient because, after a large amount of work, the new configuration will differ from the old one, essentially by a global rotation. In order to overcome this difficulty, the trick is to first choose the starting point of the cluster x_0 and then to bias the choice of the random vector r in such a way that $\sigma'(x_0)$ is close to $\sigma(x_0)$. The validity of this algorithm has been proven in Ref. 19. The program itself adjusts the bias in such a way that the average size of the cluster does not grow larger than a given fraction of the volume. The ratio $\frac{1}{3}$ gives a low autocorrelation time. The autocorrelation time for the energy is estimated by the Madras-Sokal¹⁷ automatic windowing procedure. This algorithm, in contrast to the local one, apparently shows no critical slowing down, and the computational time is improved by orders of magnitude. The program is designed for exploration work and computes many different observables, but it is not optimized for a high-precision study. We do not compute error bars on the simulation points, which make little sense anyway when used with the Ferrenberg-Swendsen method (be-

cause a point with a poor statistics may be compensated by neighbor points). By observing the effect of adding histograms into the data set, the errors are estimated to be very small, at least for first derivatives like h or D . They can be estimated by dividing the number of events in the histograms by the autocorrelation time for the energy to give the number of independent measures. The errors are then $1/\sqrt{N}$ and for all results presented here are of order of a few percent or better. The case of second derivative like C_v or χ is more demanding. Finally, the numerical difficulties should not be underestimated and the computation of the raw data takes several hundred hours of equivalent CRAY time.

IV. THE LIQUID CRYSTAL ($n=3$)

The $n=3$ case is interesting because it is a model for a film of a liquid crystal and also for numerical reasons. It is the smallest nontrivial model of the family ($n=2$ is equivalent to the XY model) and, later on, we will see that the autocorrelation time goes roughly as n . This makes the $n=3$ case the easiest to simulate, and we have studied it extensively from $L=8$ to 256. The main conclusion is that this model has a phase transition such that, below a temperature $T_c=0.358$, both the rotational rigidity modulus and the topological order parameter do not vanish. Coming from the high-temperature side, the correlation length ξ and the susceptibility χ diverge. Below T_c , it seems that both χ and ξ are infinite. The helicity modulus jumps at T_c .

In Fig. 1, we plot the different observables h , μ , D , Σ , and ξ/L vs temperature around T_c for the $L=64$ size. The most remarkable feature is the complete absence of structure of the internal energy per link h , and when looking only at this quantity we may perfectly miss the phase transition.¹⁰ We clearly have to focus on more subtle observables like μ , Σ , or ξ in order to see a clear indication of the two different phases. Figures 2 and 3 are two typical configurations for $T < T_c$ and $T > T_c$. At low

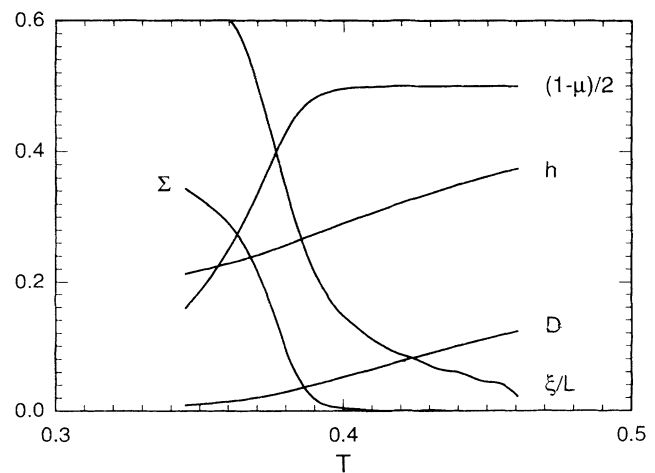


FIG. 1. The internal energy per link h , the density of defects D , the topological order parameter μ , the rotational rigidity modulus Σ , and the correlation length ξ/L vs temperature T for the RP^2 model at size $L=64$.

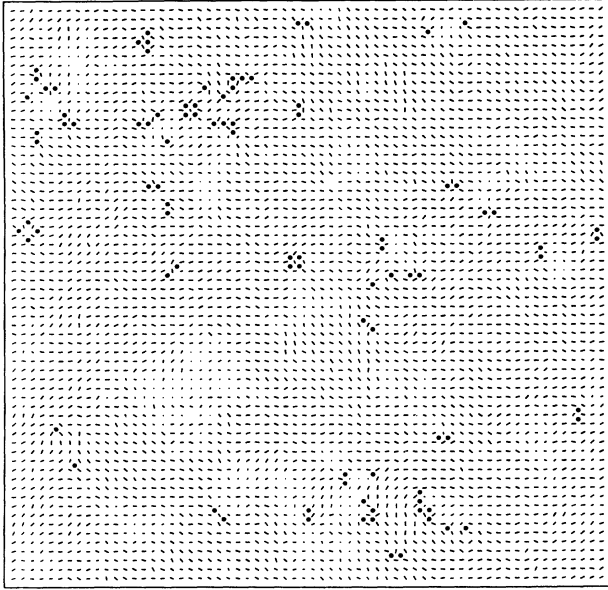


FIG. 2. A configuration for size $L=64$ and $T=0.370$. For this size, we still are in the low-temperature phase. The dash depicts the direction for $\sigma(x)$ and the dots mark plaquettes with a defect.

temperatures, defects appear in pair at distance 1, but for $T > T_c$ we observe some pairs at a larger distance or isolated defects (if pairing still makes sense at all). In Fig. 4, we represent the configuration of the energy per link for the same configuration as Fig. 2, namely, we draw the dual lattice with the surface of each link proportional to the energy of the corresponding direct space link. Links with an energy smaller than 0.2 are not represented. This is, roughly speaking, the equivalent of the Peierls contour for a model with continuous symmetry. In this figure we

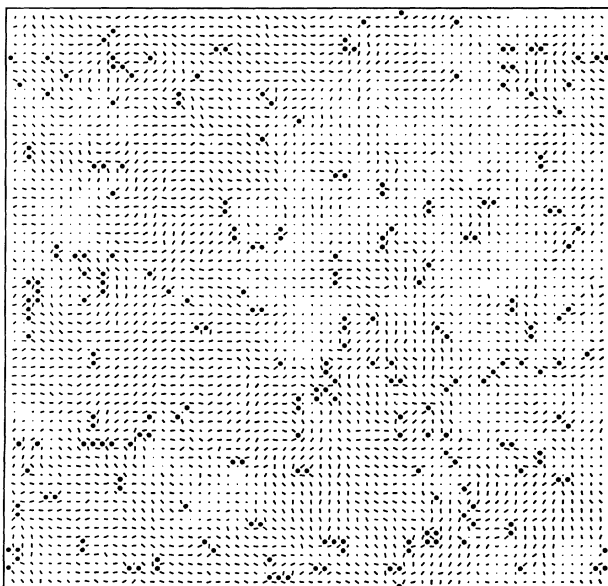


FIG. 3. As for Fig. 2, but with $T=0.400$.

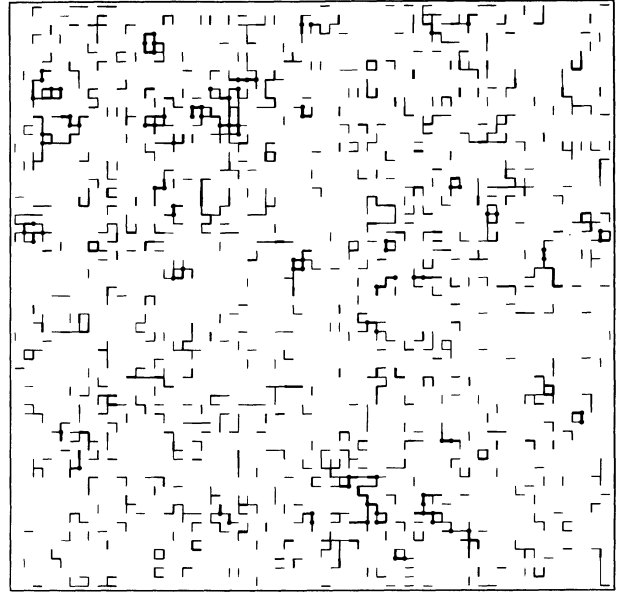


FIG. 4. The configuration of the energy for the same spin configurations as in Fig. 2 (see text).

see very clearly the importance of defects since they carry most of the energy. Also, the interaction between them is to be seen through the heavy lines joining them. Finally, the region without defects may be seen as corresponding to our intuitive idea of a spin-wave phase.

We leave the $L=64$ case in order to concentrate on scaling with the size for the various quantities. The specific heat C_v is shown in Fig. 5 for $L=8$ to 64. There is a well-defined maximum which seems to develop into a cusp when L increases, but there is clearly no divergence. This is in agreement with the previous numerical study of Chiccoli, Pasini, and Zannoni²⁰ made with the usual Metropolis algorithm. The small oscillations for $L=64$ come from the insufficient statistics in the histogram and the Ferrenberg-Swendsen method does not work properly

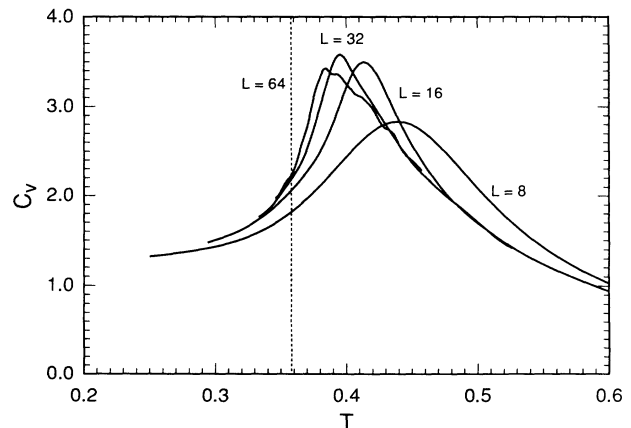


FIG. 5. The specific heat C_v vs temperature T for sizes $L=8$, 16, 32, and 64 for the RP^2 model. The dashed line is at the estimated critical temperature $T_c=0.358$, as in Figs. 7–9.

for a second-derivative quantity such as C_v .

In Fig. 6, we plot the correlation length, as well as the data for the O(3) Heisenberg model taken from Wolff.⁴ The difference is obvious, although these two models have the same naive continuum limit. We also give in Table I some of the computed data.

In order to study the approach of the transition in the high-temperature phase, we use the finite-size-scaling (FSS) hypothesis²¹ in the form

$$\begin{aligned}\xi(T,L)/L &= f(L/\xi_\infty), \\ \chi(T,L)/L &= g(L/\xi_\infty),\end{aligned}\quad (4.1)$$

where ξ_∞ denotes the infinite volume correlation length. We proceed in a similar way for the other observables with the corresponding critical exponents. In the parameter fitting, we also impose that when the correlation length is sufficiently small compared to the size of the system, the observables must tend to the infinite volume limit; that is,

$$\begin{aligned}\xi(T,L) &\rightarrow \xi_\infty \quad \text{for } \xi/L < \frac{1}{4}, \\ \chi(T,L) &\rightarrow \chi_\infty \quad \text{for } \xi/L < \frac{1}{4}.\end{aligned}\quad (4.2)$$

For the infinite volume correlation length, we try the simple power law

$$\xi_\infty = c(T - T_c)^{-\nu} \quad (4.3)$$

and the Kosterlitz-Thouless form

$$\xi_\infty = c \exp\left[\frac{a}{\sqrt{t}}\right], \quad t = (T - T_c)/T_c. \quad (4.4)$$

It is difficult to decide between these two forms. As a result, the power law fits well, but the KT form is even better. We find the values for the power law

$$\begin{aligned}T_c &= 0.356 \pm 0.002, \\ \nu &= 1.45 \pm 0.10, \\ \gamma/\nu &= 1.70 \pm 0.05, \quad \gamma = 2.45 \pm 0.1\end{aligned}\quad (4.5)$$

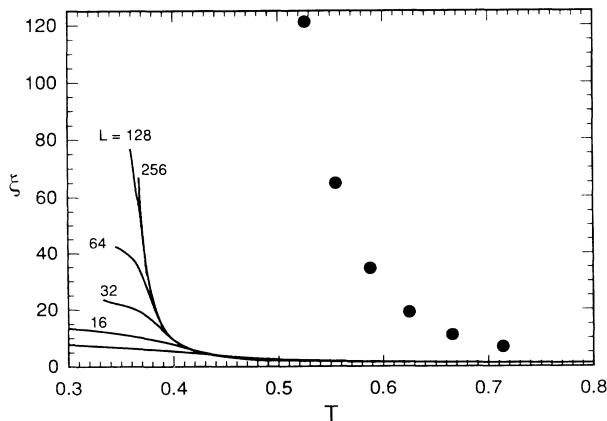


FIG. 6. The correlation length ξ vs temperature T , for the RP^2 model (solid curves) and the $\text{O}(3)=S^2$ Heisenberg model (dots) taken from Ref. 4.

TABLE I. Computed data for the RP^2 model.

L	β	ξ	χ
16	2.30	4.4	22
32	2.40	6.1	38
64	2.50	9.4	81
64	2.56	13.4	150
128	2.60	18	240
128	2.64	26	450
128	2.67	34	740
256	2.69	44	1100
256	2.71	57	1800
256	2.72	67	2300

and for the KT singularity

$$\begin{aligned}T_c &= 0.342 \pm 0.002, \\ a &= 1.57 \pm 0.05, \\ \gamma/\nu &= 1.72 \pm 0.05.\end{aligned}\quad (4.6)$$

Without any analytical hint, we would favor this second form. For example, the FSS plot for the correlation length for a KT singularity is given in Fig. 7 in a scale suited to test condition 2. Without rescaling, on the raw plot ξ vs T , the power law and KT fit are barely distinguishable from the measurements.

For the power-law singularity, these values are consistent with the theoretical computation of Solomon:¹¹ by using a Padé approximation of the high-temperature series for the continuous-time formulation of the RP^2 model, the estimation $T_c = 0.48$ and $\nu = 1.18$ is obtained. Using the scaling relation $\gamma = \nu(2 - \eta)$ and $\alpha = 2(1 - \nu)$, we deduce $\eta = 0.3$ and $\alpha = -0.65$. This negative value of α is compatible with the cusp observed in the specific heat.

It is interesting to compare these results with those of the Heisenberg model. The renormalization-group treatment in $d = 2 + \epsilon$ of both models is identical because it is sensitive only to local properties of the manifold. The

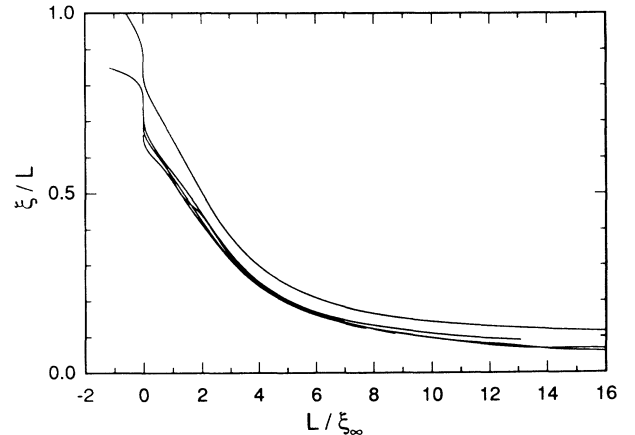


FIG. 7. The rescaled correlation length ξ/L vs L/ξ_∞ , for a KT singularity at sizes $L = 8, 16, 32, 128,$ and 256 . The parameters are $T_c = 0.342$, $a = 1.57$, $c = 0.22$.

correlation length at two-loop order is predicted to be $\xi = \xi_0(2\pi\beta)^{-1}\exp(2\pi\beta)$ (for a given size there is a crossover to a fictitious low-temperature phase and, because ξ grows very fast, one should be careful not to interpret this as a phase transition). Our attempts in that direction for the RP^2 model are clearly unsuccessful, as shown in Fig. 8 where we draw the measured correlation length divided by the above law, with β replaced by $\beta/2$, in order to recover the continuous limit. A Kosterlitz-Thouless type of divergence $\xi = \xi_0 \exp[a(T - T_c)^{-1/2}]$ does not work either. For the Heisenberg model, Wolff fits more or less successfully the previous law.⁴ The disconcerting fact is that, even with correlation lengths up to $O(100)$, there is no clear asymptotic scaling. But it is not possible to obtain a sensible fit of the Wolff data with a powerlike divergence such as (4.2).

In the low-temperature phase, scaling suggests $\chi = L^{2-\eta}$. In Fig. 9, the plot of $\ln(\chi)/\ln(L)$ vs T gives directly $2-\eta$ with approximately $\eta(T_c) = 0.4$. This is consistent with the values obtained from the high-temperature side and with the result of Ciccoli, Pasini, and Zannoni²⁰ from the power-law decay of the two-point function.

Next, we want to discuss the rotational rigidity modulus Σ and a different form of the finite-size scaling. In two dimensions and in the low-temperature phase, the correlation length will be of order L . Thus, the useful form of FSS is

$$\Sigma/\xi^{\psi/\nu} = f(\xi/L) \quad (4.7)$$

and $\xi/L > 0.6$ in the low-temperature phase, $\xi/L \rightarrow 0$ for $T > T_c$. Moreover, this form of FSS is independent of the form of ξ_∞ . In Fig. 10, we give Σ for $L = 8$ to 128, and, in the inset, the FSS plot with exponent 0. We deduced

$$\psi = 0, \quad \Sigma(T > T_c) = 0, \quad \Sigma(T < T_c) \geq 0.2. \quad (4.8)$$

This shows clearly that Σ is an order parameter for the phase transition, with a jump at T_c . An attempt to fit the data with Σ proportional to $1/\ln L$ at T_c was not successful.

Turning to topological quantities, we plot the density

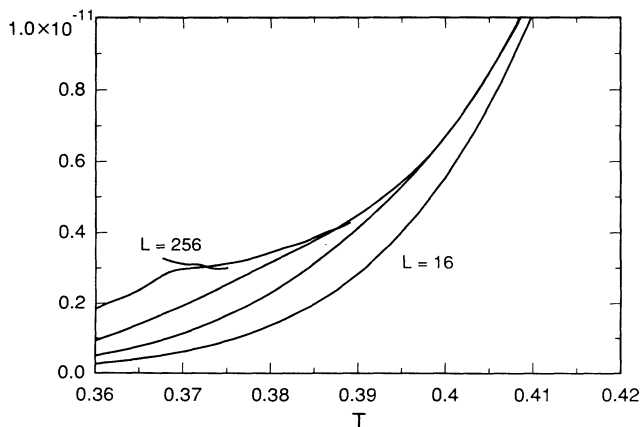


FIG. 8. The rescaled correlation length ξ . $2\pi\beta \exp(-2\pi\beta)$ vs temperature T for the RP^2 model.

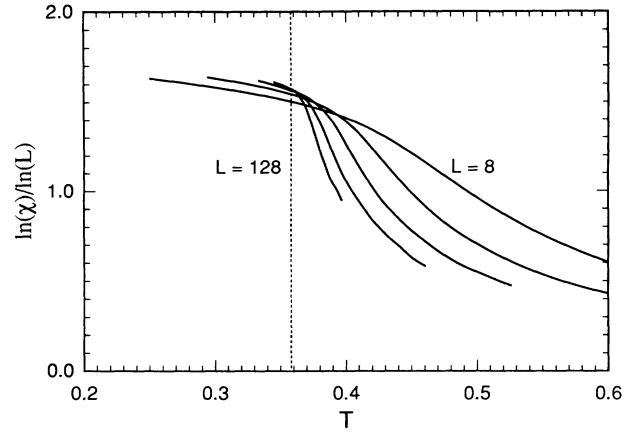


FIG. 9. The rescaled susceptibility $\ln\chi/\ln L$ vs temperature T for sizes $L = 8, 16, 32, 64,$ and 128 .

of defects D and the topological order parameter μ in Fig. 11. The density of defects shows an increase above the transition point, but there seems to be no singularity. In contrast, the results for the topological order parameter μ suggest strongly that the transition is associated to an unpairing of defects. FSS for $\partial\mu/\partial T$ suggests a transition with exponent ≈ -0.2 . This implies for $T < T_c$ that $\mu = (T_c - T)^\theta$ and $\theta \approx 0.75$. However, this value is not conclusive because, for this observable, our statistics are not sufficient.

In the low-temperature phase, we expect an activated behavior for the density of defects $D \approx \exp(-E_0/T)$. Figure 12 gives $\ln(D)$ vs β , and confirms this law with $E_0 = 0.36$. We interpret this value as the energy needed to create a pair of defects at distance $r = 1$. Close to the transition, the departure from the above law reflects the creation of pairs at distance $r > 1$. The derivative of the density of defects with respect to the temperature is given in Fig. 13. The similarity with the specific heat is striking and confirms the idea that defects play a dominant role in the transition and carry most of the energy. This suggests the existence of a singularity in $\partial D/\partial T$ with the same critical exponent as for C_v . The behavior of the density of defects is somewhat similar to that found by Lau and Dasgupta⁵ in the three-dimensional Heisenberg model. The susceptibility per unit volume for the defects χ_D is reported in Fig. 14. We see clearly how the density of defects plays the role of a disorder parameter since it shows almost no fluctuation at low temperatures, whereas it does very much at high temperatures.

Finally, we may note that the autocorrelation time of the energy, with this algorithm, has a slight maximum around the maximum of the specific heat, and grows slowly with the volume, but displays no divergence at the transition. As an order of magnitude, for size $L = 128$, the maximum autocorrelation time is $\tau = 14$ in an equivalent sweep unit. To be precise, we take as a unit Monte Carlo time when, in average, L^d spins are updated. The comparison with a traditional Metropolis algorithm will depend on the acceptance rate of this later algorithm.

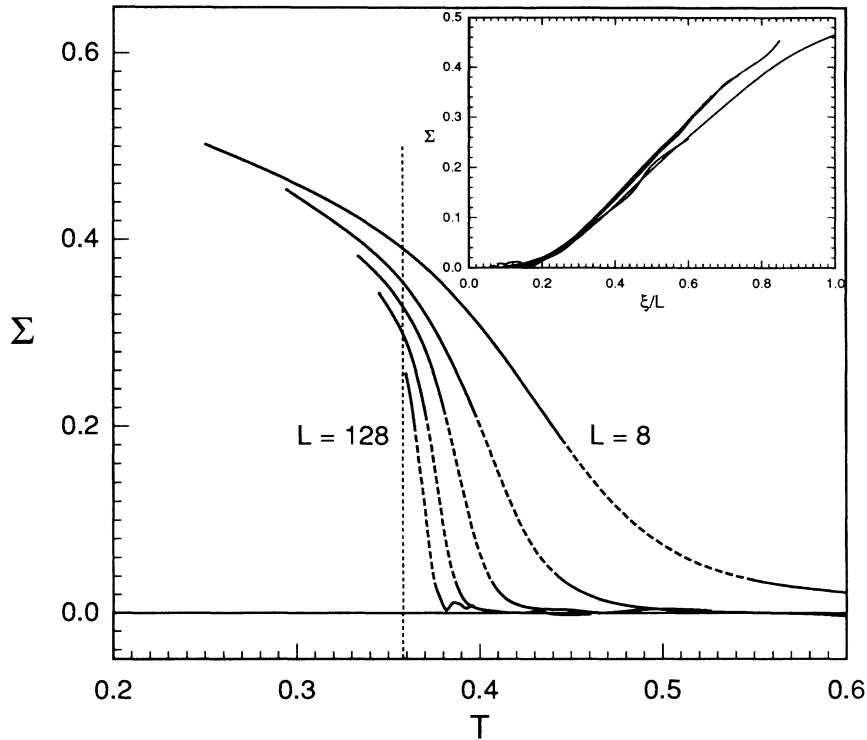


FIG. 10. The rotational rigidity modulus Σ vs temperature T for sizes $L=8, 16, 32, 64,$ and 128 for the RP^2 model. The solid lines denote the low-temperature region $\xi > L/2$ and the high-temperature region $\xi < L/4$, the dashed lines denote the crossover region $L/4 < \xi < L/2$. A FSS with exponent 0 for Σ is plotted in the inset.

V. THE LARGE- n CASE ($n=40$)

The $n=40$ case is interesting as a check for the theory near $n=\infty$. Unfortunately, as already discussed in the previous section, the difficulty grows as n , and we are able to study this problem only from $L=4$ to 32 . There are also a few simulations for $L=64$, but the statistics are clearly insufficient for the Ferrenberg-Swendsen method to work.

The results for the internal energy per link h are given

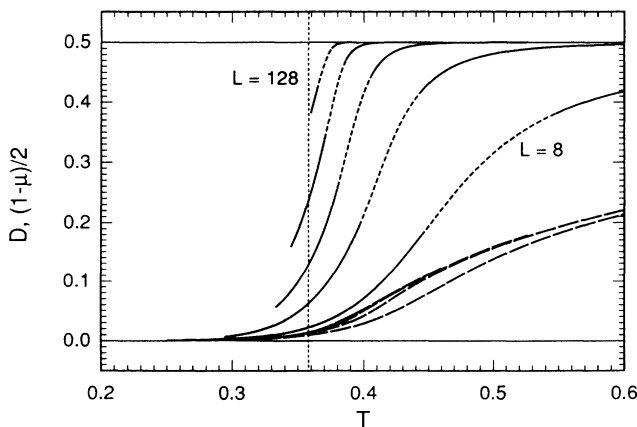


FIG. 11. The density of topological defects D (dashed lines) and the topological order parameter $(1-\mu)/2$ (solid lines) vs temperature T for sizes $L=8, 16, 32, 64,$ and 128 . Solid and dashed lines are as in Fig. 8.

in Fig. 15. For small size ($L=4, 8$), h behaves as if it would tend to a first-order transition, and it exhibits the usual signatures, i.e., a hysteresis effect with the traditional sweeping algorithm, and a double bump for the distribution of h at the transition. However, after a crossover ($L=16$), the internal energy tends to a continuous behavior for larger sizes ($L=32, 64$). Also the distribution of h displays only one peak. Nevertheless, the critical temperature $T_c=0.047$, as defined by the maximum of C_v , is not very far from the extrapolated value $T_c=0.05$ from the $n=\infty$ limit.⁷ This crossover be-

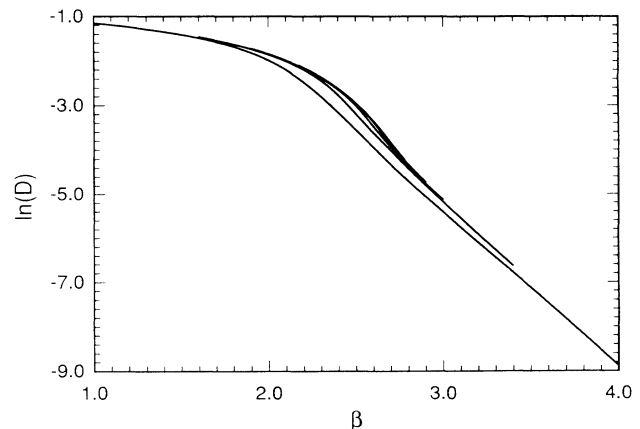


FIG. 12. The density of topological defects $\ln(D)$ vs $1/T$ for sizes $L=8, 16, 32, 64,$ and 128 .

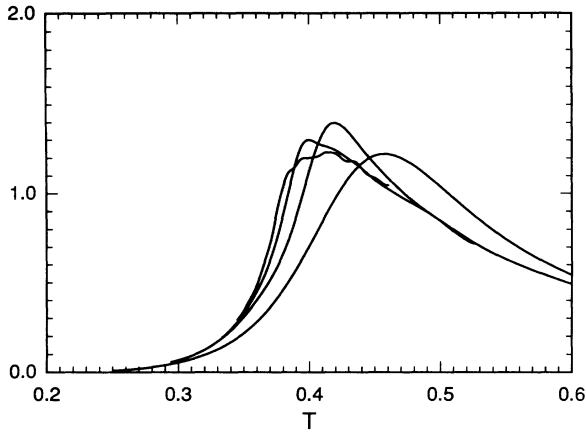


FIG. 13. The derivative of the density of defects $\partial D/\partial T$ vs T for sizes $L=8, 16, 32,$ and 64 .

tween large n and large L is observed in all quantities discussed below.

The correlation length ξ and the susceptibility χ are given in Fig. 16. There is a clear high-temperature regime where $\xi \approx 1$ and $\chi \approx 1$. The critical temperatures correspond to the end of this regime. Below T_c , there is first a linear increase with T of ξ and χ , followed by a saturation. Contrary to the $n=3$ case, this saturation is not fixed by the lattice size (for example, at $\xi \approx L/2$), but much below. Also, χ grows slower than some power of L , but rather like ξ^2 . This seems to indicate that the correlation length remains finite below T_c , even if our lattice sizes are too small to give the precise value. This behavior has to be compared with the $n=\infty$ limit, where $\xi=1$ for $T > T_c$, and ξ very large but finite for $T < T_c$.

The rotational rigidity modulus Σ is given in Fig. 17. This shows that, even in the low-temperature region, Σ seems to vanish as the size of the system grows, in agreement with the analysis for $n=\infty$.

The topological quantities D and μ are reported in Fig. 18. The behavior is similar to the case $n=3$, indicating

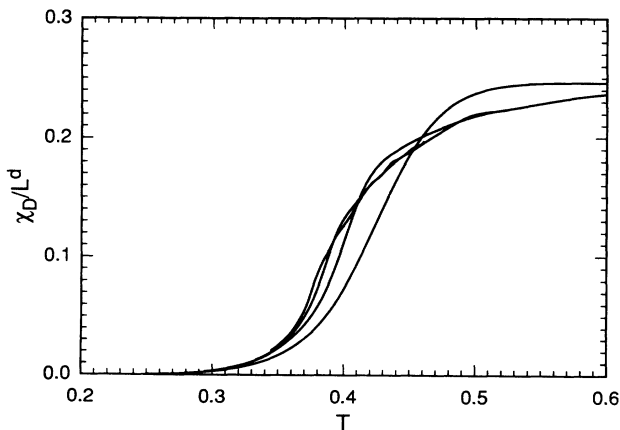


FIG. 14. The susceptibility per unit volume for the defects χ_D/L^d vs T for size $L=8, 16, 32,$ and 64 for the RP^2 model.

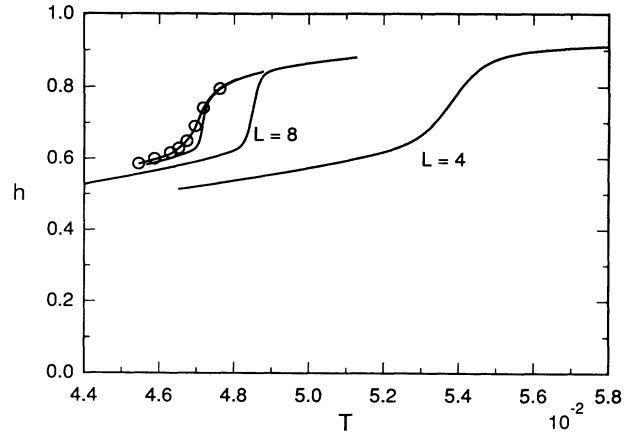


FIG. 15. The internal energy per link h vs temperature T for sizes $L=4, 8, 16, 32,$ and 64 for the RP^{39} model. For size 64 , the statistic is insufficient for the Ferrenberg-Swendsen method to work and the dots correspond to simulations, as for Figs. 14–18.

that the transition is associated to the unbinding of defects. The search for an activated law for D in the low-temperature phase is given in Fig. 19, and we obtain the value $E_0 \approx 5$. This value is different from the $n=3$ case, reflecting the fact that spin waves and defects are coupled in the RP^{n-1} model. The susceptibility of defects per unit volume, as given in Fig. 20, clearly marks the two different phases. The number of defects fluctuates very strongly as we approach the critical temperature, in contrast to the $n=3$ case.

Finally, the autocorrelation time τ for the energy shows a slow increase with the size of the system, and a clear increase around the critical temperature, but seems not to diverge. The order of magnitude for size $L=64$ is between 250 and 2000 in an equivalent sweep unit.

In conclusion, for this large- n simulation, we clearly observe two different regimes, similar to the $n=\infty$ analysis, but the precise nature of the transition between them remains elusive. It seems not to be of first order, as defined by a jump of the internal energy, and not to be of second order, as defined by a divergence of the correlation length. How can we understand the fact that a phase transition seems to occur for large n , at a critical temperature T_c given by the $n=\infty$ limit, but that its nature is not correctly described by that limit? We have rigorously proved that, for the free energy, the thermodynamic limit and the $n=\infty$ limit can be interchanged, justifying an assumption made in Ref. 7. This implies when n is very large that the internal energy of the infinite system is given correctly by its $n=\infty$ limit for all temperatures except possibly near $T_c(n=\infty)$. We may suspect that, for finite n , in a neighborhood of T_c of size $1/n$, these two limits cannot be exchanged. The crossover effects observed numerically also indicate that, in two dimensions, the two limits cannot be interchanged for the correlation functions. In contrast, in three dimensions they can, since a first-order transition already appears for $n=3$.

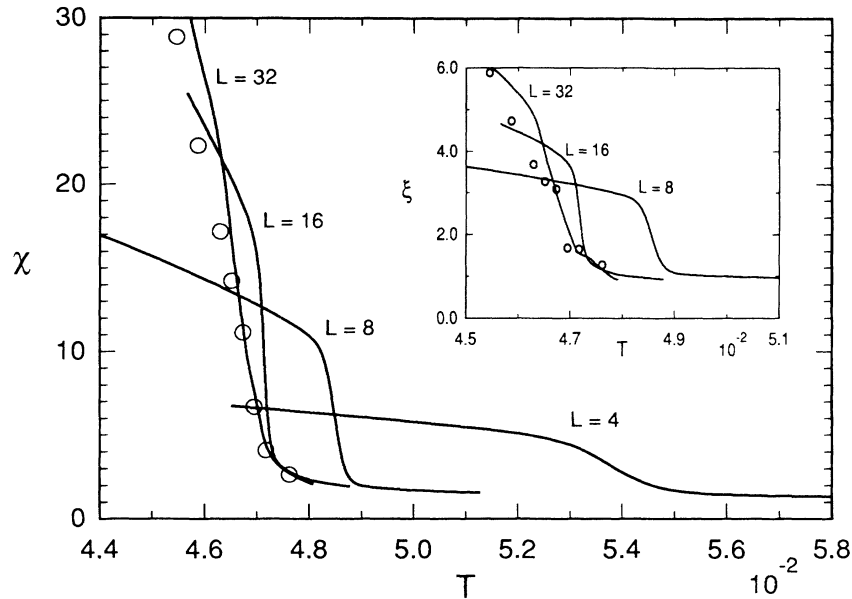


FIG. 16. The susceptibility χ and the correlation length ξ vs temperature T for the RP^{39} model.

VI. THE GENERAL n CASE

A scan for small size through the various models for different n shows a continuous change with n . For large n , the critical temperatures, taken as the maximum of C_v , scale as $T_c \approx n/2$, in agreement with the $n = \infty$ limit. On the opposite side, we can extrapolate the curve $T_c(n)$ down to $n = 0$, with $T_c(0) \approx 1$. However, we have no interpretation for this model.

The comparison of the autocorrelation time τ for various n shows that $\tau \approx n$. This can be understood as coming from the fact that we need n draws of the random vector r to really explore RP^{n-1} and to generate an independent configuration. This is why the simulation for large n is much more difficult.

VII. CONCLUSIONS

We have presented various corroborating pieces of evidence for a topological phase transition in the two-

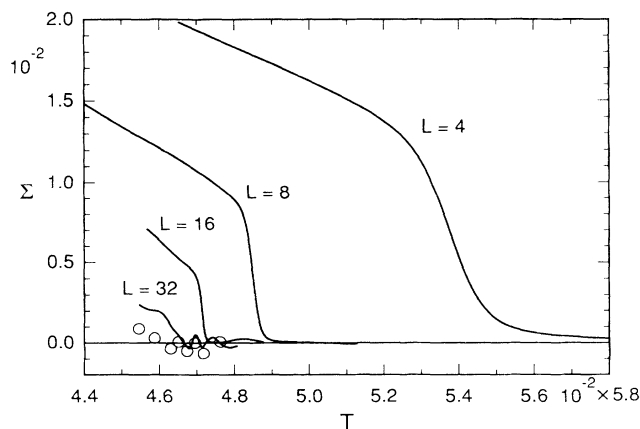


FIG. 17. The rotational rigidity modulus Σ vs temperature T for sizes $L = 4, 8, 16, 32,$ and 64 for the RP^{39} model.

dimensional RP^{n-1} model. The numerical results demonstrate that defects and their interactions are the leading mechanism for this transition. It would be highly desirable to construct an effective Hamiltonian which would describe the interaction of these defects. This is a rather difficult task because this interaction should be of the many-body type. Indeed, the law of addition of their charge implies that, sufficiently far apart, two defects will always look as no defect at all. This should be contrasted with the interaction of vortices in the XY model, and might explain the differences observed between the two transitions, despite some common features, the most notable ones being a divergent correlation length and susceptibility at low temperatures and a discontinuity in an order parameter. However, it should be kept in mind that a numerical result is certainly not a proof.

On the more analytical side, we can dispose of the

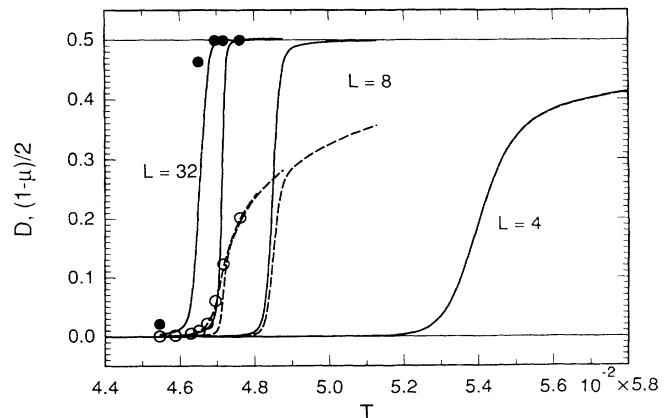


FIG. 18. The density of topological defects D (dashed line) and the topological order parameter $(1-\mu)/2$ (solid line) vs temperature T for sizes $L = 4, 8, 16, 32,$ and 64 .

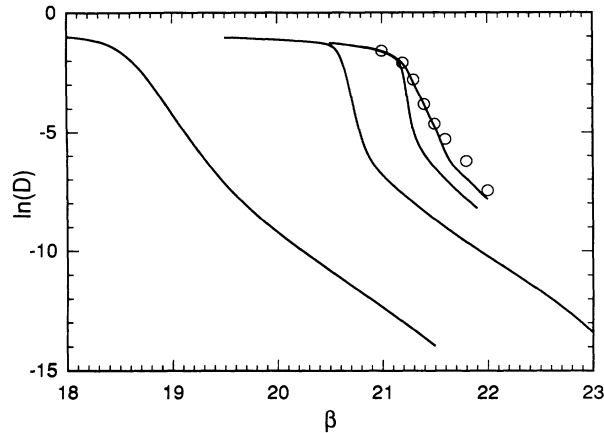


FIG. 19. The density of topological defects $\ln(D)$ vs $1/T$ for sizes $L = 4, 8, 16, 32,$ and 64 .

large- n limit. Although we saw that this limit correctly gives the critical temperature but does not reproduce the observed nature of the transition. This unsuspected phenomenon might be cause for concern in the study of other models, for which a $1/n$ expansion is the only theoretical tool at the investigator's disposal.

Finally, we think that these results can explain the puzzle posed by the $2 + \epsilon$ expansion applied to RP^{n-1} , which predicts incorrectly a continuous transition in three dimensions when a first-order one is observed. Indeed, we have presented evidence of a phase transition at positive temperature already in two dimensions.

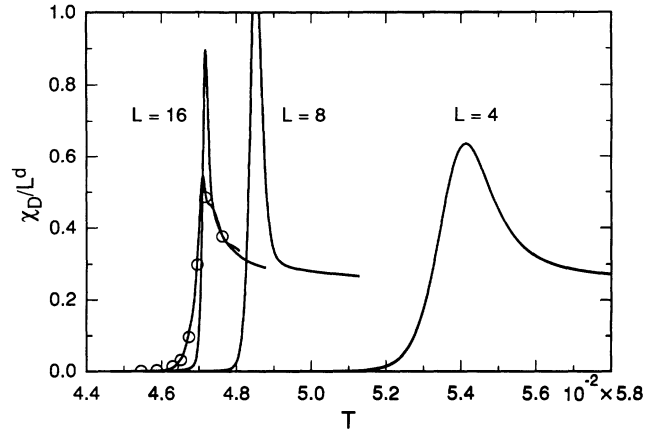


FIG. 20. The susceptibility per unit volume for the defects χ_D/L^d vs T for sizes $L = 4, 8, 16, 32,$ and 64 for the RP^{39} model.

ACKNOWLEDGMENTS

This work was partly supported by the Fonds National Suisse de la Recherche Scientifique. G.Z. wants to acknowledge the hospitality of l'Università di Roma, Tor Vergata, and useful discussions with A. Beretti, E. Marinari, E. Biffet, and K. Efetov. Programs were run at l'Università di Roma, l'Ecola Polytechnique Fédérale de Lausanne, and the Max-Planck-Institut in Stuttgart. We thank all these institutions for their support. We thank U. Wolff for a useful discussion about the use of bias in Monte Carlo simulations.

- ¹V. Berezinskii, Zh. Eksp Teor. Fiz. **59**, 907 (1970) [Sov. Phys. JETP **32**, 493 (1971)].
²J. M. Kosterlitz and D. J. Thouless, J. Phys. C **6**, 1181 (1973).
³A. M. Polyakov, Phys. Lett. **59B**, 79 (1975).
⁴U. Wolff, Phys. Lett. B **222**, 473 (1989).
⁵M. Lau and C. Dasgupta, Phys. Rev. B **39**, 7212 (1989).
⁶P. A. Lebwohl and G. Lasher, Phys. Rev. A **6**, 426 (1972).
⁷H. Kunz and G. Zumbach, J. Phys. A **22**, L1043 (1989).
⁸J. Zinn-Justin, *Quantum Field Theory and Critical Phenomenon* (Oxford Science, New York, 1989).
⁹U. Fabbri and C. Zannoni, Mol. Phys. **58**, 763 (1986).
¹⁰S. Duane and M. Green, Phys. Lett. **103B**, 359 (1981).
¹¹S. Solomon, Phys. Lett. **100B**, 492 (1981).
¹²U. Wolff, Phys. Rev. Lett. **62**, 361 (1989); Nucl. Phys. **B322**, 759 (1989).

- ¹³S. Solomon, Y. Stavans, and E. Domany, Phys. Lett. **122B**, 373 (1982).
¹⁴A. Ferrenberg and R. Swendsen, Phys. Rev. Lett. **61**, 2635 (1988); **63**, 1195 (1989).
¹⁵F. Wegner, Z. Phys. B **35**, 207 (1979).
¹⁶H. Kunz and G. Zumbach, Phys. Lett. B **257**, 299 (1991).
¹⁷N. Madras and A. D. Sokal, J. Stat. Phys. **50**, 109 (1988).
¹⁸M. E. Fischer, M. N. Barber, and D. Jasnow, Phys. Rev. A **8**, 1111 (1973).
¹⁹G. Zumbach and H. Kunz, Phys. Lett. A (to be published).
²⁰C. Ciccoli, P. Pasini, and C. Zannoni, Physica A **148**, 298 (1988).
²¹*Finite Size Scaling*, edited by J. L. Cardy (North-Holland, Amsterdam, 1988).